

Efforts to monitor and characterize the recent increasing seismicity in central Oklahoma

D. E. McNamara¹, J. L. Rubinstein², E. Myers¹, G. Smoczyk¹, H. M. Benz¹, R. A. Williams¹, G. Hayes¹, D. Wilson³, R. Herrmann⁴, N. D. McMahon⁵, R. C. Aster⁵, E. Bergman⁶, A. Holland⁷, and P. Earle¹

Abstract

The sharp increase in seismicity over a broad region of central Oklahoma has raised concerns regarding the source of the activity and its potential hazard to local communities and energy-industry infrastructure. Efforts to monitor and characterize the earthquake sequences in central Oklahoma are reviewed. Since early 2010, numerous organizations have deployed temporary portable seismic stations in central Oklahoma to record the evolving seismicity. A multiple-event relocation method is applied to produce a catalog of central Oklahoma earthquakes from late 2009 into early 2015. Regional moment tensor (RMT) source parameters were determined for the largest and best-recorded earthquakes. Combining RMT results with relocated seismicity enabled determination of the length, depth, and style-of-faulting occurring on reactivated subsurface fault systems. It was found that the majority of earthquakes occur on near-vertical, optimally oriented (northeast-southwest and northwest-southeast), strike-slip faults in the shallow crystalline basement. In 2014, 17 earthquakes occurred with magnitudes of 4 or larger. It is suggested that these recently reactivated fault systems pose the greatest potential hazard to the region.

Introduction

It is well established that in 2009 the earthquake rate significantly increased throughout the central United States and that it is not an artifact of improved seismic-network monitoring capabilities (Ellsworth, 2013; Ellsworth et al., this issue). More than 50% of these earthquakes since 2009 have occurred in central Oklahoma, and in the past few years (2013–2015), earthquake rates have increased even more, thus raising concerns for potential hazard to local communities and energy-industry infrastructure in central Oklahoma (McNamara et al., 2015).

Here we review collaborative efforts by the United States Geological Survey (USGS), the Oklahoma Geological Survey (OGS), the University of Oklahoma (OU), Oklahoma State University (OSU), and the Incorporated Research Institutions in Seismology (IRIS) to monitor and characterize the evolving earthquake sequences in central Oklahoma. We describe ongoing seismic station deployments, quantify the recent earthquake rate increase, compute detailed earthquake source parameters, and place constraints on the spatial distribution of reactivated fault zones (Figure 1). Based on characteristics of the November 2011 Prague M_w 5.6 earthquake sequence, we suggest that 12 separate recently reactivated fault systems pose the greatest potential hazard to the region (Figure 1). Results from this study are an update of McNamara et al. (2015) and can contribute to the

assessment of earthquake hazard for the short-term traffic-light system implemented by the Oklahoma Corporation Commission (OCC) and the long-term USGS National Seismic Hazard Map (NSHM) (Petersen et al., 2014, 2015; Ellsworth et al., this issue).

Recent increase in Oklahoma seismicity

The recent increase in seismicity is illustrated best as the rate changes observed in cumulative seismic moment versus time (Figure 2), which show a steady increase in cumulative moment from 2009 to late 2011. In 2011, a sharp step in cumulative-moment release occurred because of the Prague sequence in November 2011, which includes an M_w 5.6 and three $M_w > 4$ earthquakes. Following the Prague sequence, cumulative-moment release rose moderately until late 2013, when it began to rise sharply because of a significant increase in the number of higher-magnitude earthquakes over an expanded region of active seismicity (McNamara et al., 2015) (Figures 1 and 2). In 2014, 608 magnitude 3 and greater earthquakes occurred in central Oklahoma (more than in the state of California), including 17 earthquakes with magnitudes of 4 or larger (a rate of 1.4/month). This year, 2015, shows

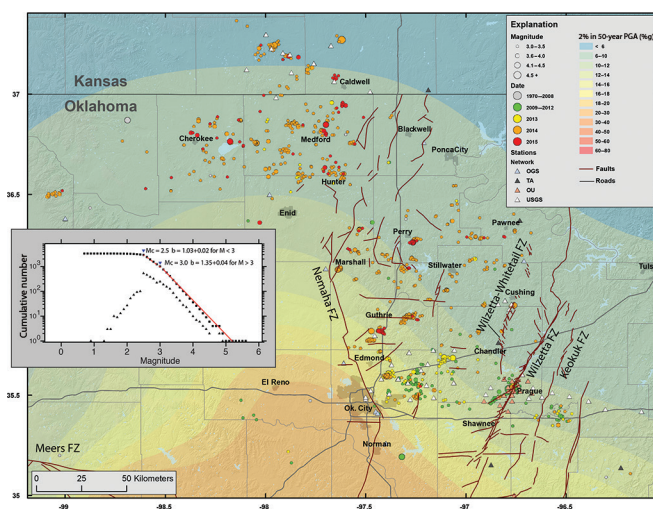


Figure 1. Map showing the original ($M \geq 3$) USGS NEIC single-event epicenters from 1974 through February 2015, colored by year and sized by magnitude. Color contours represent peak ground acceleration (in percent g) with 2% probability of being exceeded in 50 years from the 2014 update of the USGS National Seismic Hazard Map (Petersen et al., 2014). Brown lines are known subsurface faults from numerous sources (Miser, 1954; Bennison, 1964; Chenoweth, 1983; Joseph, 1987; Northcutt and Campbell, 1995; McBee, 2003). The inset panel shows the magnitude of completeness ($M_c = 3$) and b -value fit for the catalog from 1974–2015.

¹U. S. Geological Survey, National Earthquake Information Center.
²U. S. Geological Survey.
³U. S. Geological Survey, Albuquerque Seismological Laboratory.
⁴Department of Earth and Atmospheric Sciences, St. Louis University.

⁵Department of Geosciences, Colorado State University.
⁶Global Seismological Services.
⁷Oklahoma Geological Survey.
DOI information...

no sign of decline in earthquake rate, with more than 200 M 3 and nine M 4 earthquakes by late March — a rate of three M 4 and larger earthquakes per month (Figure 2).

Rubinstein et al. (2014) show that the earthquake rate change observed in the Raton Basin of Colorado and New Mexico is highly improbable for random fluctuations in a constant background. We applied the same methods to a declustered catalog of $M \geq 3.2$ earthquakes in central Oklahoma and southern Kansas (Figure 1) and found that for any individual year since the earthquake rates increased (i.e., 2009–2014), the rates observed in that year are highly improbable, given an earthquake catalog from 1974 through that year (probability maximum $P_{\max} = 0.03$). The same test applied to 2007 and 2008 yields $P_{\max} = 0.65$ for both years, indicating that given earlier seismicity, the rates observed during these years were likely. Using the previous year to predict the seismicity shows that the earthquake rates in 2009, 2013, and 2014 are highly improbable ($P_{\max} = 0.03$, $P_{\max} = 0.0007$, and $P_{\max} = 0.00004$, respectively), indicating that earthquake rates increased significantly in those years. For the years 2010–2012, the rates

observed weren't improbable ($P_{\max} = 0.28$, $P_{\max} = 0.99$, $P_{\max} = 0.50$, respectively), indicating that the earthquake rate didn't change significantly in those years relative to the previous year's rate. The observed earthquake-rate increase, combined with an increase in earthquake clustering in time (Llenos and Michael, 2013), indicates that a fundamental change in the earthquake-triggering process has occurred (McNamara et al., 2015).

Since settlement of the region, Oklahoma has a well-documented history of felt earthquakes. Prior to the recent increase in seismicity, the largest event in central Oklahoma were two earthquakes in the range of magnitude 5 (10 September 1918 and 08 April 1952) (Von Hake, 1976; Luza and Lawson, 1982). Paleoseismology studies have identified the Meers fault as a Holocene thrust fault with a surface rupture and scarp located in south-central Oklahoma, and a history of earthquakes dating back over 1100 years (Luza et al., 1987). In contrast, recent Oklahoma seismicity is well to the northeast of the Meers fault zone, and distributed over a much broader region of ancient reactivated structures associated with the Nemaha and Wilzetta fault zones (Figure 1).

The 2014 update of the USGS NSHM did not include most of the recent seismicity, and as a consequence, the highest predicted shaking in Oklahoma is well to the southwest and centered on earthquakes that occurred on the Meers fault zone (Figure 1). The recent earthquakes were not included because several studies have raised suspicion that they are induced because of anthropogenic activity (Holland, 2013; Keranen et al., 2013; Llenos and Michael, 2013), and therefore long-term earthquake hazard in central Oklahoma is currently underestimated (Figure 1) (Petersen et al., 2014).

USGS earthquake monitoring and characterization efforts

A significant scientific issue for the USGS earthquake-hazard program is to consider how to incorporate the recent earthquakes in central Oklahoma in the calculation of the NSHM (Petersen et al., 2015; Ellsworth et al., this issue; McGarr et al., 2015; (McNamara et al., 2015)). The USGS National Earthquake Information Center (NEIC) is responsible for characterizing felt earthquakes in the United States and throughout the world. This characterization includes rapid determination of hypocenter location, magnitude estimation, moment tensors, fault-rupture modeling and impact assessment (USGS Prompt Assessment of Global Earthquakes for Response [PAGER]). In addition, earthquake source parameters determined by the USGS NEIC are used to determine long-term earthquake hazard throughout the United States (Petersen et al., 2014). The USGS is currently working on several fronts to understand better the mechanisms driving the earthquake rate increase and estimate the changing earthquake hazard in Oklahoma (Keranen et al., 2014; Hough, 2014; Sumy et al., 2014; Sun and Hartzell, 2014; Ellsworth et al., this issue; McNamara et al., 2015; Petersen et al., 2015; H. M. Benz, R. McMahon, D. Aster, D. McNamara, and D. Harris, personal communication, 2015).

Oklahoma seismic-station deployments

Beginning in early 2010, the USGS in cooperation with the Oklahoma Geological Survey began deploying temporary portable strong-motion seismic stations to the northeast of Oklahoma City to improve monitoring of the increasing seismicity and potentially

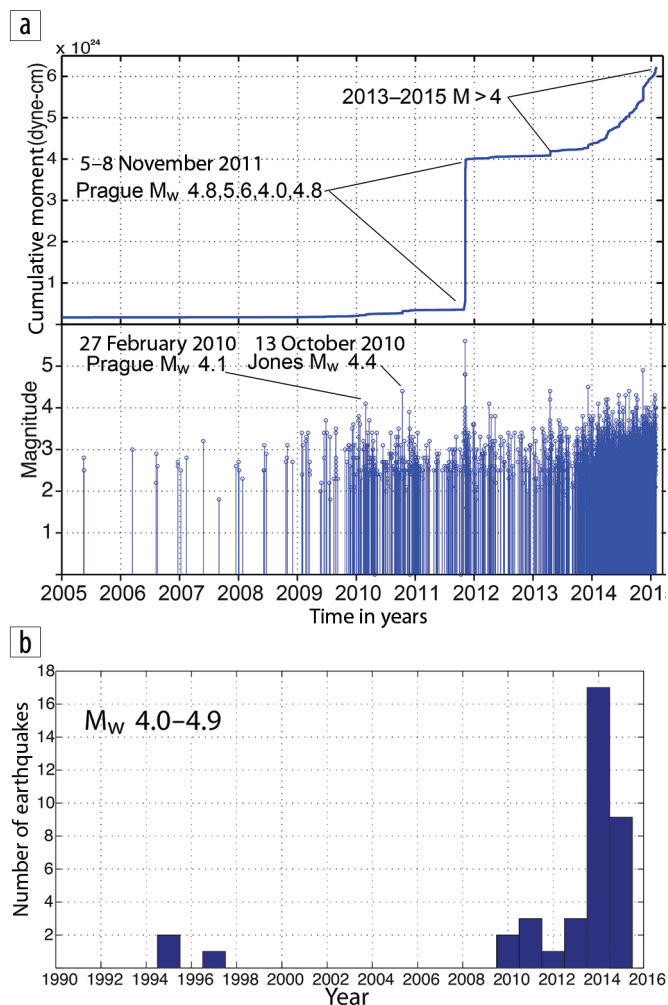


Figure 2. Central Oklahoma earthquake characteristics from the USGS COMCAT online system. (a) Earthquakes from the NEIC COMCAT system from 2005 through February 2015. Plot showing cumulative moment release (top panel). Timeline showing earthquake magnitude versus time (bottom panel). (b) The number of magnitude 4 earthquakes per year from 1990–2015.

to capture ground shaking from a large event (Figure 1). Immediately following the M_w 4.8 earthquake of 5 November 2011 in the Prague region, the University of Oklahoma (OU) rapidly installed three broadband seismograph stations near the epicenter of the earthquake. These stations were deployed in time to record the M_w 5.6 Prague earthquake on the following day (5 November 2011) (Keranen et al., 2013; McNamara et al., 2015). The unprecedented occurrence of two significant earthquakes in the area prompted the USGS and IRIS to assist OU and the OGS in the deployment of additional seismograph stations. Field teams from OU added an additional five seismograph stations within three days of the main shock, while IRIS completed the installation of 10 stations by 9 November 2011. In the same timeframe, the USGS added three combined strong-motion/broadband stations in the epicentral area and ten broadband stations in an approximately 100-km-long pseudolinear array (Sumy et al., 2014).

Since the November 2011 Prague sequence, numerous additional stations have been deployed by OGS and the USGS to monitor the northwest migration of seismicity (Figure 1). In 2013–2014, the USGS deployed stations in southern Kansas have contributed to improved earthquake-monitoring capability in northern Oklahoma (Rubinstein et al., 2014). Complementing the portable deployments were temporary, regionally distributed stations in the Earthscope Transportable Array, and permanent stations operated by the OGS seismic network (McNamara et al., 2015) and the USGS Advanced National Seismic System (ANSS) backbone network. The combined network of permanent and temporary seismic-station deployments provided high-quality waveforms in real time to the USGS NEIC for seismic phase picks that are analyzed routinely in real time to determine detailed earthquake-source parameters that can be used to characterize regions of reactivated faulting in central Oklahoma (McNamara et al., 2015).

NEIC earthquake characterization

NEIC single-event hypocenter determination. Earthquake source characteristics (hypocenter location, depth, and magnitude) for most detectable earthquakes ($M > 2.5$) in the United States are routinely computed at the USGS NEIC and displayed online at <http://earthquakes.usgs.gov>. Initial earthquake locations were determined with a standard “single-event” approach using a stand-alone version of the main real-time processing and analysis system used by the USGS NEIC (Buland et al., 2009). This system allowed us to identify and locate individual earthquakes, compute network-averaged regional magnitudes (e.g., M_L , m_bL_g , M_d), and M_w from RMT waveform modeling of earthquakes larger than approximately M 3.5.

A three-step approach was used for initial processing of the waveform data. First, all publicly available waveform data were loaded into an instance of the USGS NEIC operational processing system. Earthquake P -wave and S -wave phases were picked automatically and associated into common events, and source parameters (location, magnitude) were determined. Second, the automatic locations and magnitudes were reviewed manually to improve the seismic phase arrival-time picks and to add new secondary phases as available. This primarily included first arriving S -waves that the automatic process did not identify. Finally, the continuous waveform data were reviewed visually to find small events that the

automatic process missed. Seismic phase traveltimes were computed using the AK135 one-dimensional global velocity model (Kennett et al., 1995). We did not locate all observed earthquakes — only those events for which there was a sufficient number of arrival-time observations and good azimuthal coverage to ensure a well-constrained hypocenter. Typically, smaller earthquakes were recorded on only a few stations, making it difficult to determine location and depth accurately. For regions in which a dense network of seismic stations was available (Guthrie, Cushing, Prague), subspace detection was applied to lower the magnitude of completeness (H. M. Benz, R. McMahon, D. Aster, D. McNamara, and D. Harris, personal communication, 2015).

Hypocentroidal decomposition multiple-event relocation. After initial single-event earthquake locations and magnitudes were determined using the procedures described above, they were reanalyzed to refine further source locations using a multiple-event approach based on the hypocentroidal decomposition algorithm (HD) (Jordan and Sverdrup, 1981).

Hypocentroidal decomposition is a multiple-event procedure in the same class of methods that include joint hypocentral determination (Dewey, 1972) and double difference (Waldhauser and Ellsworth, 2000). The HD relocation method provides improved hypocenter locations with minimized location bias and realistic estimates of location uncertainty for each earthquake (McNamara et al., 2015). When a dense network of local seismic stations is available (Prague, Guthrie, and Cushing), location uncertainty is reduced to < 1 km (McNamara et al., 2015). In other regions where only a few stations are located within 10–20 km (Cherokee, Stillwater, Medford, and Renfro), uncertainty is reduced to < 2 km (Figure 3). In addition, relocating earthquakes using HD can reduce, by a factor of two, the scatter in hypocenter locations determined using single-event methods (Figure 3). Another advantage of this method is the ability to relocate a poorly recorded main shock by tying it to clusters of aftershocks that often are recorded

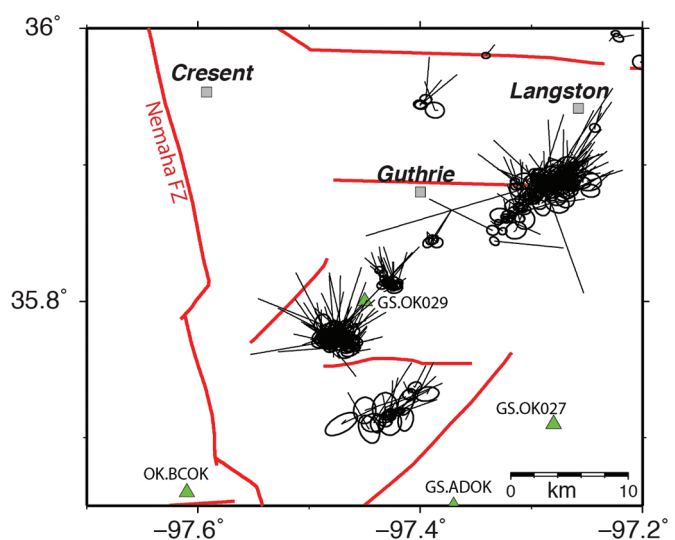


Figure 3. Uncertainty ellipses and location change vectors for earthquakes in the sequences near Guthrie and Langston. Green triangles show portable seismometers deployed to monitor the seismicity in the region. Structures associated with the Nemaha fault zone are shown as red lines.

on a dense local network (McNamara et al., 2015). These advantages have motivated the USGS NEIC to implement multiple-event hypocenter location methods to improve hypocenter accuracy and uncertainty for earthquake sequences of interest to the nation.

The map in Figure 3 shows the uncertainty ellipses of the epicenters and the direction and length of the change in locations relative to the final HD location for recent (2013–2014) seismicity near Guthrie and Langston, Oklahoma. Epicentral errors are reduced significantly relative to the original NEIC single-event location. Good constraints on older epicentral locations can be attributed directly to well-constrained locations of more recent earthquakes recorded at both the temporary and permanent stations in the area, which establish the traveltimes corrections needed to relocate these events properly. In the Guthrie–Langston sequences, station density is not as high as in the other regions (Prague, Cushing, and Jones) so uncertainty ellipses are generally larger (> 1.0 km). Recent examples of HD applications and method details can be found in Hayes et al. (2013), Hayes et al. (2014), McNamara et al. (2014), Rubinstein et al. (2014), and McNamara et al. (2015).

Regional moment tensors. Focal mechanism solutions for U. S. earthquakes are computed routinely at the USGS NEIC for $M > 3.5$ earthquakes, using the RMT method described in Herrmann et al. (2011) (Figure 4). Successful waveform modeling of regional body and surface waves depends upon selecting a frequency band in which the signal-to-noise ratio is high and filtered waveforms are relatively simple, which requires evaluation of the RMT modeling for each earthquake. With few exceptions, we find that most Oklahoma regional earthquakes that are regionally well recorded (generally with $M > 3.5$) can be modeled in the period band 16–50 s. This period band is below the microseismic noise, with periods that are long enough to minimize effects from scattering, but short enough to improve depth estimates. Green’s functions were computed using the western U. S. model of Herrmann et al. (2011), a model that fits the observed local and regional P-wave traveltimes and surface-wave amplitude and dispersion in the period band 10–100 s for Oklahoma earthquakes. RMT calculations provide good estimates of the earthquake depth, magnitude, and faulting style (McNamara et al., 2015), allowing characterization of reactivated fault structures that pose the greatest hazard to the region.

Reactivated structures pose a potential hazard to communities and infrastructure

The specific earthquake sequences observed in central Oklahoma in recent years do not behave with a typical main-shock-aftershock progression. Instead, they are swarm-like, similar to volcanic sequences, with large and small magnitude events interspersed in time, and most of the larger earthquakes are preceded by numerous moderate foreshocks. The November 2011 Prague, Oklahoma, sequence is a good example, with an equal number of magnitude 4 foreshocks and aftershocks.

Combined analysis of the spatial distribution of multi-event relocated seismicity and RMT focal-mechanism nodal planes allows us to place constraints on the location, orientation, and style of reactivated fault structures. The majority of the recent earthquakes in central Oklahoma occur along reactivated ancient subsurface faults at shallow depths in the crust (< 6 km); these faults

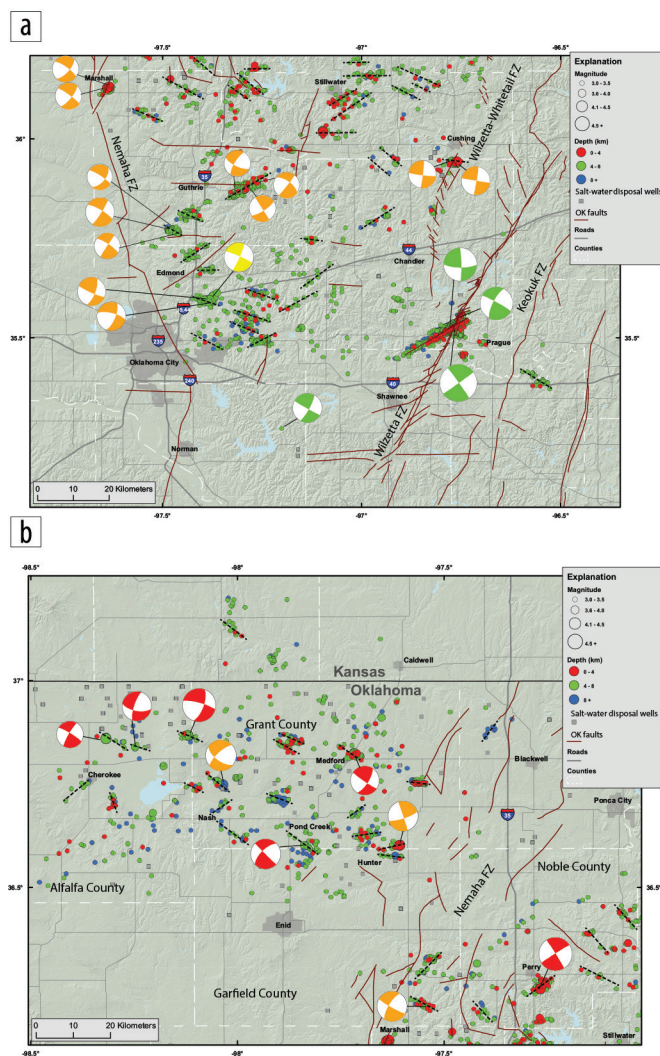


Figure 4. Central Oklahoma regional maps. Earthquakes relocated by hypocentroidal decomposition (HD) are shown as circles colored by depth and sized by magnitude. Also shown are known subsurface faults (solid brown lines), inferred faults (dashed black lines) and injection wells (gray squares). Subsurface faults are inferred from the combined analysis of the spatial distribution of seismicity and focal mechanism nodal planes. Also shown are RMT focal mechanisms for earthquakes with $M_w \geq 4$. Regional moment tensors are colored by year (green occurred in 2012–2013, yellow in 2013, orange in 2014, and red in 2015). (a) South-central Oklahoma, including the Oklahoma City metropolitan area and the Nemaha–Wilzetta uplift region. (b) North-west-central Oklahoma region including Alfalfa and Grant counties.

cut through the Cambro–Ordovician Arbuckle Group and extend down into the crystalline basement (McNamara et al., 2015). In some cases, earthquake sequences are associated clearly with known fault systems. In most cases, the earthquake sequences occur away from known faults but align within a similar fabric. Figure 4 shows subsurface faults inferred from the combined analysis of the spatial distribution of seismicity and focal-mechanism nodal planes as dashed black lines; however, for clarity only RMT focal mechanisms for earthquakes with $M_w \geq 4$ are mapped.

The RMT focal mechanisms determined in central Oklahoma are predominantly strike-slip with one nodal plane oriented north-east to southwest and the other oriented northwest to southeast

(McNamara et al., 2015) (Figure 4). A small number of RMTs, in the Prague and Cushing sequences, have nodal planes that strike east-west and north-south. The three dominant RMT nodal plane orientations are aligned approximately with the known subsurface fault fabric identified in numerous geologic maps and reports (Miser, 1954; Bennison, 1964; Chenoweth, 1983; Joseph, 1987; Northcutt and Campbell, 1995; McBee, 2003). Most RMT nodal planes are oriented optimally relative to the approximately east-west maximum horizontal compression direction for reactivating earthquake activity on ancient faults (Holland, 2013; Alt and Zoback, 2014; McNamara et al., 2015).

Since the earthquake rate increase in 2009 to early 2015, there has been a clear southeast to northwest migration of the seismically active regions (Figure 1), twelve of which have produced earthquakes with magnitudes greater than 4 (Figure 4). Based on characteristics of the November 2011 Prague M_W 5.6 earthquake sequence (Keranen et al., 2013; McNamara et al., 2015) and the circumstances detailed below, we suggest that recently reactivated fault systems with earthquakes greater than magnitude 4 pose the greatest potential hazard to communities and infrastructure in the region.

Earthquake sequences in south-central Oklahoma along the Nemaha and Wilzetta fault zones

South-central Oklahoma is the most populated region of the state with over one million inhabitants in the Oklahoma City metropolitan area. It is also the location of significant energy industry and national strategic infrastructure such as the Cushing crude-oil storage facility. Earthquake sequences in this region are associated with the Nemaha and Wilzetta fault zones that bound a broad region of uplift originally formed as a result of the Ancestral Rocky Mountains orogeny during the Pennsylvanian period (Figure 4a) (Joseph, 1987; Luza and Lawson, 1982). The uplifted region is a complex belt of ancient, buried high-angle faults that hosts reservoirs of oil and gas (Dolton and Finn, 1989; McNamara et al., 2015). Most recent earthquake sequences occurred on reactivated conjugate strike-slip structures that are structurally similar to reactivated faults that produced the 2011 Prague, Oklahoma, (M_W 5.6) earthquake sequence.

November 2011 Prague earthquake sequence. The M_W 5.6 Prague earthquake of 06 November 2011 was the largest earthquake in Oklahoma recorded history. It was felt widely in the neighboring states of Texas, Arkansas, Kansas, and Missouri, and as far away as Tennessee and Wisconsin. The M_W 5.6 earthquake was preceded by many foreshocks, including an M_W 4.0 in February 2010 and an M_W 4.8 (05 November 2011) earthquake the previous day. The sequence also included two $M \geq 4.0$ aftershocks (M_W 4.0 on 6 November 2011 and M_W 4.8 on 8 November 2011). The USGS PAGER system (U. S. Geological Survey, 2011) estimated that more than 3000 people in an area of approximately 65 km² in the immediate vicinity of the M_W 5.6 epicenter experienced severe shaking of intensity levels MMI VIII = 34–65%g.

Shaking in the epicentral region was significantly stronger than peak acceleration shaking levels predicted in the 2014 USGS NSHM when suspected induced earthquakes were not included in the model (2% probability of exceedance in 50 years = 10–12%g,

MMI V–VI) (Petersen et al., 2014) (Figure 1) and more consistent with shaking levels when all earthquakes are included (0.04% probability of exceedance in one year = 50–200%g MMI VIII–X) (Petersen et al., 2015; Ellsworth et al., this issue). This shaking destroyed six houses, 20 homes sustained major damage (averaging \$80,000 per home for repairs), and 38 homes had minor damage (estimated repair costs of \$13,000 per home) (Branstetter and Killman, 2015). Fortunately, the earthquake sequence occurred in a relatively sparsely populated region of central Oklahoma and widespread damage was avoided; however, several residents are pursuing reimbursement currently for damage to their homes through the Oklahoma state court system (Wertz, 2015).

The sequence of earthquakes occurred at a complex intersection of conjugate strike-slip faults within the Wilzetta fault zone (Figure 4a) (McNamara et al., 2015). This intersection of reactivated fault segments within the Wilzetta fault zone includes a relatively long (approximately 20 km) main branch, along with several shorter (2–4 km) conjugate structures. The RMT analysis for the M_W 4.8 foreshock and M_W 5.6 main shock defines a near-vertical northeast striking nodal planes with right-lateral, strike-slip mechanism that aligns with trends in the relocated seismicity (Figure 4a). The 08 November 2011 M_W 4.8 aftershock also has a near-vertical, strike-slip mechanism, but is left lateral with an east-west striking nodal plane that aligns with an approximately 5-km splay of aftershock seismicity. The seismicity and focal mechanisms combined indicate activity on conjugate strike-slip faults, likely activated in response to the stress changes from the cascading sequence of earthquakes (Sumy et al., 2014; McNamara et al., 2015).

Elevated hazard for Oklahoma City. Beginning in 2010 and continuing to the time of writing (late February 2015), earthquake rates have shown a significant increase in the region northeast of Oklahoma City. The HD relocation hypocenters define several discrete sequences with linear trends consistent with the general fabric of known faults within the Nemaha and Wilzetta fault zones (Figure 4a). Most relocated earthquake depths (3–8 km) are within the Arbuckle disposal formation and in the deeper basement structures (McNamara et al., 2015).

Of particular concern for residents of Oklahoma City are active earthquake sequences associated with long fault structures that might be capable of supporting large earthquakes (M 5–6). Examples include the approximately 12-km-long sequence east of Guthrie (Figure 4a), the sequence south of Marshall along a reactivated segment of the Nemaha fault zone, and smaller sequences throughout the region that might be connected at depth to optimally oriented splays of the Nemaha fault zone (McNamara et al., 2015) (Figure 4a). As defined by the recent seismicity, the uplifted region between the Nemaha and Wilzetta fault zones hosts numerous previously unknown associated subfaults, that if connected at depth to the main branch of the Nemaha fault zone, could cause a cascade of earthquakes in the same manner as the Prague sequence in November 2011 (Sumy et al., 2014). An earthquake of similar magnitude to the Prague M_W 5.6 would produce severe shaking in a broad region around the epicenter (MMI VIII) and would pose significant hazard to the higher-population-density region of the Oklahoma City metropolitan area.

October 2014 Cushing earthquake sequence: Elevated hazard for national strategic infrastructure. In October 2014, two moderate-sized earthquakes (M_W 4.0 and 4.3) struck immediately south of Cushing, Oklahoma, 5 km beneath the site of the largest crude-oil storage facility in the conterminous United States and a major hub of the U. S. oil-and-gas pipeline transportation system (Pipeline and Hazardous Materials Safety Administration, 2015). The earthquakes occurred on an unnamed, left-lateral strike-slip fault that intersects with other recently reactivated segments of the right-lateral Wilzetta-Whitetail fault zone (Bennison, 1964; McBee, 2003) (Figure 4a). Minor damage was reported throughout the city of Cushing, including cracked plaster, broken window glass, and items thrown from shelves.

Shortly after the 7 October 2014 Cushing M_W 4.0 event, the OCC halted injection operations at three wells within a six-mile radius around the main-shock epicenter. This was the first implementation of the OCC's traffic-light system since inception in late 2013. Inspectors found that the Wildhorse wastewater-disposal well was injecting into the basement, below the disposal formation (Arbuckle), which, because of the likely presence of subsurface faults, can increase greatly the potential for inducing earthquakes (Zoback, 2012; Ellsworth, 2013). The Wildhorse disposal well was ordered by the OCC to halt operations and plug with cement back up to the depth of the Arbuckle formation. Two additional wells in the vicinity (Calyx, Wilson) also experienced short periods of halted operations following the largest earthquakes in the Cushing sequence. Once injection operations resumed, two days following shutdown and plug in, the sequence drastically died off with no recorded earthquakes since late November 2014. With the plummeting price of crude oil, the Cushing storage facility is expected to approach peak capacity (80 million barrels) by April 2015 (Wilmoth, 2015), exposing critical resources and infrastructure to elevated earthquake hazard. The OCC implementation of the traffic-light system has been a success so far in this case for mitigating potential damage to the Cushing facility and possibly avoiding an environmental disaster for the residents of nearby Cushing, Oklahoma, and costly cleanup for the energy industry.

Recent seismicity in northwest central Oklahoma. Northwest central Oklahoma has experienced the most recent seismicity as a result of northwest migration of active earthquake sequences (Figures 1 and 4b). The recent earthquakes are dispersed over several northern Oklahoma counties (Alfalfa, Grant, Garfield, and Noble) with sequences of most potential hazard ($M_W \geq 4$) located near the towns of Perry, Medford, and Cherokee (Figure 4b). In 2013, Alfalfa County had only three earthquakes with a maximum M_W of 2.8, while Grant County to the east experienced approximately 35, with a maximum magnitude of M_W 3.6. In 2014, as wastewater injection increased to some of the highest levels in state (Soraghan, 2015), the frequency and magnitude of local earthquakes greatly increased, introducing the first $M > 4.0$ earthquakes to these northern counties (M_W 4.0 and M_W 4.3 in Grant County) (Figure 4b).

This trend continued into February 2015, with 48 earthquakes in Alfalfa County and 85 in Grant County since the beginning of the year. Grant County has already experienced

three earthquakes of at least M_W 4.0, as has Alfalfa County, each within 20 km of Cherokee and operational wastewater disposal wells. The most recent of these larger events occurred within six days of each other, January 30th and February 5th, within 10 km of Cherokee. Following the M_W 4.0 on 30 January 2015, injection operations at the SandRidge Energy Miguel well were halted. This marks the second implementation of the OCC traffic-light system. Less than a week after this decision was made, a second large earthquake occurred (M_W 4.2), less than 8 km away from the first, with multiple, smaller accompanying aftershocks.

Similar to the active earthquake sequences near Oklahoma City, RMT nodal planes align with trends in the relocated seismicity and define a series of near-vertical, reactivated strike-slip faults. The reactivated structures are a mix of northwest-to-southeast-striking left-lateral and northeast-to-southwest-striking right-lateral strike-slip faults that generally align with the regional fabric of the Nemaha fault zone (Figure 4a). Earthquake sequences near Perry and Marshall clearly are associated clearly with the Nemaha fault zone. In contrast, earthquake sequences farther to the west near the towns of Medford and Cherokee (McNamara et al., 2015) occur away from known faults but align within a similar general fabric observed throughout central Oklahoma. The combined analysis of RMTs and relocated earthquake sequences enables the characterization of these previously unknown and unmapped fault structures that pose elevated hazard to communities and infrastructure in the region.

Conclusions

Traditionally, it has been difficult to develop spatial correlations between earthquakes and specific faults in the central United States. This has resulted primarily from low seismicity rates and few well-constrained earthquake locations and moment-tensor solutions. The combination of the recent increased earthquake rate and good seismic-station coverage over a broad region of central Oklahoma allowed us to build a catalog of calibrated earthquake hypocenters and regional-moment-tensor solutions. Combining RMT results with relocated seismicity enabled us to determine the length, depth, and style of faulting occurring on reactivated subsurface fault systems.

Using the catalog of earthquake-source parameters determined in this study, we delineate numerous reactivated subsurface faults throughout central Oklahoma and are working to provide guidance on which faults pose the highest hazard. The majority of the reactivated faults in the region are oriented favorably for earthquake rupture relative to the regional compressive stress field. Earthquakes are shallow and constrained primarily to the upper portion of the crystalline basement (a depth of less than 6 km), with some seismicity reaching into the overlying sedimentary bedrock. Many of the earthquakes relocated in this study coalesce from diffuse and scattered locations into discontinuous sequences with fault lengths of 1–12 km. Most of these discontinuous sequences are aligned consistently with the general fabric of the Nemaha and Wilzetta fault zones, but we are uncertain about whether there are longer fault structures tying together these independent clusters. Many earthquake sequences are associated directly with well-known structures of

the Nemaha and Wilzetta fault zones. However, most earthquakes occur in the broad region of uplift and are not associated with known fault zones.

Recently, the Oklahoma Geological Society and the Oklahoma Corporation Commission have been collaborating on building an enhanced fault database for Oklahoma. This type of product will be valuable for understanding the faulting process and will help mitigation efforts. Access to proprietary well and reflection data also could aid in understanding the relationship between recent seismicity and reactivated fault zones. In addition, new OCC regulations on reporting and monitoring of wastewater disposal wells will help improve our understanding of the earthquake process. These are necessary first-order observations required to assess the potential hazards of individual faults in Oklahoma. Results from this study are important parameters required to assess both short-term (traffic-light) and long-term (NSHM) earthquake hazard. We suggest that the increased rate and occurrence of earthquakes near optimally oriented and long fault structures has raised the earthquake hazard in central Oklahoma and increased the probability for a damaging earthquake. ■■

Acknowledgments

This research was supported by the United States Geological Survey's National Earthquake Hazards Reduction Program. We thank R. Herrmann and NEIC analysts for RMT parameters determined in this study, which are available to research scientists and engineers from the USGS COMCAT system (<http://earthquake.usgs.gov/>). All waveform data used in this study, from both portable and permanent seismic stations, are archived and available for download from the IRIS Data Management Center (DMC). The ZMAP software was used for earthquake FMD and Omori's law calculations (Wiemer, 2001). R. Herrmann, N. McMahan, and R. Aster contributed code and analysis on several projects. The authors greatly appreciate the hard work of people who have responded to the evolving sequences. The USGS field crews included A. Leeds, J. Allen, S. Roberts, D. Worley, M. Meremonte, and E. Cochran. We also would like to thank staff at IRIS PASSCAL, Oklahoma State University, and the Oklahoma Geological Survey for material and logistical support. D. Ketchum provided easy access to waveform and metadata. We also thank the NEIC analysts for initial single-event locations and phase picks.

Corresponding author: mcnamara@usgs.gov

References

Alt, R. C., and M. D. Zoback, 2014, Development of a detailed stress map of Oklahoma for avoidance of potentially active faults when siting wastewater injection wells: 2014 Fall Meeting, AGU, Abstract S51A-4434.

Bennison, A., 1964: The Cushing Field, Creek County, Oklahoma: Tulsa Geological Society Digest, **32**, 158–159.

Branstetter, Z., and Killman, C., 2015, Earthquake politics: 'We don't work in a vacuum,' Oklahoma state seismologist says (10 February 2015): Tulsa World, http://www.tulsaworld.com/earthquakes/earthquake-politics-we-don-t-work-in-a-vacuum-oklahoma/article_9cea5c50-246a-5f6d-8b98-3b7979430ca6.html, accessed 20 February 2015.

Buland, R. P., M. Guy, D. Kragness, J. Patton, B. Erickson, M. Morrison, C. Bryan, D. Ketchum, and H. Benz, 2009, Comprehensive seismic monitoring for emergency response and hazards assessment: Recent developments at the USGS National Earthquake Information Center: 2009 Fall Meeting, AGU, Abstract S11B-1696.

Chenoweth, P. A., 1983, Principal structural features of Oklahoma (map): PennWell.

Dewey, J., 1972, Seismicity and tectonics of western Venezuela: Bulletin of the Seismological Society of America, **62**, 1711–1751.

Dolton, G. L., and T. M. Finn, 1989, Petroleum geology of the Nemaha Uplift, central Midcontinent: USGS Open-File Report 88-450D.

Ellsworth, W. L., 2013, Injection-induced earthquakes: Science, **341**, no. 6142, 142–149, <http://dx.doi.org/10.1126/science.1225942>.

Ellsworth, W. L., A. L. Llenos, A. F. McGarr, A. J. Michael, and J. L. Rubinstein, 2015, Increasing seismicity in the U. S. midcontinent: Implications for earthquake hazard: The Leading Edge, this issue.

Hayes, G. P., E. Bergman, K. L. Johnson, H. M. Benz, L. Brown, and A. S. Melzer, 2013, Seismotectonic framework of the 2010 February 27 M_w 8.8 Maule, Chile earthquake sequence: Geophysical Journal International, **195**, no. 2, 1034–1051, <http://dx.doi.org/10.1093/gji/ggt238>.

Hayes, G. P., M. W. Herman, W. D. Barnhart, K. P. Furlong, S. Riquelme, H. M. Benz, E. Bergman, S. Barrientos, P. S. Earle, and S. Samsonov, 2014, Continuing megathrust earthquake potential in Chile after the 2014 Iquique earthquake: Nature, **512**, no. 7514, 295–298, <http://dx.doi.org/10.1038/nature13677>.

Herrmann, R. B., H. M. Benz, and C. J. Ammon, 2011, Monitoring the earthquake source process in North America: Bulletin of the Seismological Society of America, **101**, 2609–2625, <http://dx.doi.org/10.1785/0120110095>.

Holland, A. A., 2013, Optimal fault orientations within Oklahoma: Seismological Research Letters, **84**, 876–890, <http://dx.doi.org/10.1785/0220120153>.

Hough, S., 2014, Shaking from injection-induced earthquakes in the central and eastern United States: Bulletin of the Seismological Society of America, **104**, 2619–2626, <http://dx.doi.org/10.1785/0120140099>.

Jordan, T. H., and K. A. Sverdrup, 1981, Teleseismic location techniques and their application to earthquake clusters in the south-central Pacific: Bulletin of the Seismological Society of America, **71**, 1105–1130.

Joseph, L., 1987, Subsurface analysis, "Cherokee" Group (Des Moinesian), portions of Lincoln, Pottawatomie, Seminole, and Okfuskee Counties, Oklahoma: The Shale Shaker, **12**, 44–69.

Kennett, B. L. N., E. R. Engdahl, and R. Buland, 1995, Constraints on seismic velocities in the earth from traveltimes: Geophysical Journal International, **122**, 108–124, <http://dx.doi.org/10.1111/j.1365-246X.1995.tb03540.x>.

Keranen, K. M., H. M. Savage, G. A. Abers, and E. S. Cochran, 2013, Potentially induced earthquakes in Oklahoma, USA: Links between wastewater injection and the 2011 M_w 5.7 earthquake sequence: Geology, **41**, 699–702, <http://dx.doi.org/10.1130/G34045.1>.

Keranen, K. M., M. Weingarten, G. A. Abers, B. A. Bekins, and S. Ge, 2014, Sharp increase in central Oklahoma seismicity since 2008 induced by massive wastewater injection: Science, **345**, 448–451, <http://dx.doi.org/10.1126/science.1255802>.

Llenos, A. L., and A. J. Michael, 2013, Modeling earthquake rate changes in Oklahoma and Arkansas: Possible signatures of

- induced seismicity: *Bulletin of the Seismological Society of America*, **103**, 2850–2861, <http://dx.doi.org/10.1785/0120130017>.
- Luza, K. V., and J. E. Lawson Jr., 1982, Seismicity and tectonic relationships of the Nemaha uplift in Oklahoma, part IV: Oklahoma Geological Survey, Special Publication 82-1, http://www.ogs.edu/pubsscanned/SPs/SP82_1.pdf, accessed 20 February 2015.
- Luza, K. V., R. F. Madole, and A. J. Crone, 1987, Investigation of the Meers fault in southwestern Oklahoma: Nuclear Regulatory Commission, NUREG/CR-4937.
- McBee, W., 2003, Nemaha strike-slip fault zone: Mid-Continent Section Meeting, AAPG, Abstract.
- McGarr, A., B. Bekins, N. Burkardt, J. Dewey, P. Earle, W. Ellsworth, S. Ge, S. Hickman, A. Holland, E. Majer, J. Rubinstein, and A. Sheehan, 2015, Coping with earthquakes induced by fluid injection: *Science*, **347**, 830–831, <http://dx.doi.org/10.1126/science.aaa0494>.
- McNamara, D. E., H. M. Benz, R. B. Herrmann, E. A. Bergman, P. Earle, A. Holland, R. Baldwin, and A. Gassner, 2015, Earthquake hypocenters and focal mechanisms in central Oklahoma reveal a complex system of reactivated subsurface strike-slip faulting: *Geophysical Research Letters*, <http://dx.doi.org/10.1002/2014GL062730>.
- McNamara, D. E., H. M. Benz, R. B. Herrmann, E. A. Bergman, and M. Chapman, 2014, The M_w 5.8 central Virginia seismic zone earthquake sequence of August 23, 2011: Constraints on earthquake source parameters and fault geometry: *Bulletin of the Seismological Society of America*, **104**, 40–54.
- Miser, H. D., 1954, Geologic map of Oklahoma: U. S. Geological Survey.
- Northcutt, R. A., and J. A. Campbell, 1995, Geological provinces of Oklahoma: Oklahoma Geological Survey Open-File Report OF5-95.
- Petersen, M. D., M. P. Moschetti, P. M. Powers, C. S. Mueller, K. M. Haller, A. D. Frankel, Y. Zeng, S. Rezaeian, S. C. Harmsen, O. S. Boyd, N. Field, R. Chen, K. S. Rukstales, N. Luco, R. L. Wheeler, R. A. Williams, and A. H. Olsen, 2014, Documentation for the 2014 update of the United States national seismic hazard maps: U. S. Geological Survey Open-File Report 2014-1091.
- Petersen, M. D., C. S. Mueller, M. P. Moschetti, S. Hoover, J. L. Rubinstein, W. L. Ellsworth, A. Holland, and J. G. Anderson, 2015, Incorporating induced seismicity in the 2014 United States national seismic hazard models — Results of 2014 workshop and Sensitivity studies: U. S. Geological Survey Open-File Report 2015-1070, <http://dx.doi.org/10.3133/ofr20151070>.
- Pipeline and Hazardous Materials Safety Administration, 2015, National pipeline mapping system: <https://www.npms.phmsa.dot.gov>, accessed 20 February 2015.
- Rubinstein, J. L., W. L. Ellsworth, A. McGarr, and J. Benz, 2014, The 2001–present induced earthquake sequence in the Raton Basin of Northern New Mexico and Southern Colorado: *Bulletin of the Seismological Society of America*, **104**, 1–20, <http://dx.doi.org/10.1785/0120140009>.
- Rubinstein, J., W. L. Ellsworth, A. L. Llenos, and S. R. Walter, 2014, Is the recent increase in seismicity in southern Kansas natural?: 2014 Fall Meeting, AGU, S53E–8.
- Sorghan, M., 2015, Research shows strong correlation between quakes, oil activity (9 February 2015): *EnergyWire*, <http://www.eenews.net/stories/1060013080>, accessed 20 February 2015.
- Sumy, D. F., E. S. Cochran, K. M. Keranen, M. Wei, and G. A. Abers, 2014, Observations of static Coulomb stress triggering of the November 2011 $M_{5.7}$ Oklahoma earthquake sequence: *Journal of Geophysical Research Solid Earth*, **119**, no. 3, 1904–1923, <http://dx.doi.org/10.1002/2013JB010612>.
- Sun, X., and S. Hartzell, 2014, Finite-fault slip model of the 2011 M_w 5.6 Prague, Oklahoma earthquake from regional waveforms: *Geophysical Research Letters*, **41**, 4207–4213, <http://dx.doi.org/10.1002/2014GL060410>.
- U. S. Geological Survey, 2011, PAGER – M 5.6 – Oklahoma: <http://earthquake.usgs.gov/earthquakes/pager/events/us/b0006klz/index.html>, accessed 20 February 2015.
- Von Hake, C. A., 1976, Oklahoma earthquake history: *Earthquake Information Bulletin*, **8**, 28–30.
- Waldhauser, F., and W. L. Ellsworth, 2000, A double-difference earthquake location algorithm: Method and application to the northern Hayward fault, California: *Bulletin of the Seismological Society of America*, **90**, no. 6, 1353–1368, <http://dx.doi.org/10.1785/0120000006>.
- Wertz, J., 2015, Oklahoma Supreme Court to decide lawsuit over earthquake near Prague, Okla. (26 January 2015): *State Impact (NPR)*, <http://stateimpact.npr.org/oklahoma/2015/01/26/oklahoma-supreme-court-to-decide-lawsuit-over-earthquake-near-prague-okla/>, accessed 20 February 2015.
- Wiemer, S., 2001, A software package to analyze seismicity: ZMAP: *Seismological Research Letters*, **72**, no. 3, 373–382, <http://dx.doi.org/10.1785/gssrl.72.3.373>.
- Wilmoth, A., 2015, Crude oil pouring into Cushing, Oklahoma: Billions of dollars worth of oil is arriving for storage at the Oklahoma town dubbed “pipeline crossroads of the world” (20 February 2015): *The Oklahoman*, <http://newsok.com/article/5394908>, accessed 20 February 2015.
- Zoback, M. D., 2012, Managing the seismic risk posed by wastewater disposal: *Earth Magazine*, **57**, 38–43.